



Clinical Efficacy of Novel Elastography Using Acoustic Radiation Force Impulse (ARFI) for Diagnosis of Malignant Thyroid Nodules

Takahiro Fukuhara, MD, PhD ; Eriko Matsuda, MPAS; Ryohei Donishi, MD;
Satoshi Koyama, MD, PhD ; Naritomo Miyake, MD, PhD; Kazunori Fujiwara, MD, PhD;
Hiromi Takeuchi, MD, PhD

Objective: Acoustic radiation force impulse (ARFI) imaging is a recent ultrasound elastography technique; consequently, its efficacy is not fully known. In this study, we compared ARFI imaging with conventional strain elastography (SE) and shear wave velocities (SWVs) to evaluate the utility of ARFI imaging for diagnosing thyroid nodules.

Subjects and Methods: In this study we examined 233 thyroid nodules (183 benign nodules and 50 malignant nodules) isolated from human patients. The nodules were evaluated with SE and ARFI imaging, and SWVs of the nodules were simultaneously measured. ARFI images were classified using a four-point score based on grayscale intensity of the images. The sensitivity, specificity, and diagnostic accuracy were compared between SE and ARFI imaging. Finally, SWVs for each score of SE and ARFI imaging were compared.

Results: The new scoring system for ARFI imaging can be divided into four virtual touch imaging (VTI) scores. Nodules with a VTI score of 3 or 4 as determined by ARFI imaging were determined to be malignant. The sensitivity, specificity, and diagnostic accuracy, respectively, were 63.2%, 66.3%, and 65.6% for SE, compared with 80.0%, 86.3%, and 85.0% for ARFI imaging. The median SWVs of the nodules were 1.57 m/s, 1.73 m/s, 1.88 m/s, and 2.09 m/s for VTI scores of 1, 2, 3, and 4, respectively. The SWVs of VTI scores 3 and 4 were significantly higher than those of VTI scores 1 and 2.

Conclusions: The diagnostic accuracy of ARFI imaging for differentiating malignant thyroid nodules was higher than that of SE. The VTI scores of the nodules accurately reflected their SWVs.

Key Words: ARFI, ultrasonography, elastography, thyroid nodule, shear wave.

Level of Evidence: 4

INTRODUCTION

Elastography is a novel application of using ultrasound to assess tissue elasticity. Lyshchik et al. first reported the clinical application of elastography to the characterization of thyroid tumors in 2005.¹ The conventional form of elastography is strain elastography (SE), which assesses the elasticity of tissues by measuring the extent of tissue strain generated by manual compression. The extent of strain is represented using a color map, indicating tissue elasticity.

However, this form of elastography uses manual compression and is operator-dependent. Therefore, the accuracy of the SE relies on the operator's skill and

experience^{2,3} and has been reported to result in highly variable outcomes.⁴⁻⁹

Several years ago, a novel elastography method using acoustic compression became commercially available. There are two types of novel elastography that use acoustic radiation force impulse (ARFI): ARFI imaging, a type of SE, and quantitative shear wave elastography (SWE).

ARFI imaging assesses tissue elasticity from the amount of displacement of the tissue. This is generated by an acoustic push pulse, which displaces the target tissue locally, and can displace the whole target tissue with numerous acoustic push pulses. The extent of tissue displacement is expressed in grayscale. Solid tissues are represented by black and soft tissues by white. We hypothesize that this method can objectively assess the local elastic characteristics of target tissues.

The other quantitative method, SWE, assesses tissue elasticity by measuring the velocity of the shear wave generated by ARFI. The shear wave velocity (SWV) reflects tissue elasticity, as calculated by Young's modulus.¹⁰ Thus, SWE can be used to evaluate tissue stiffness, both quantitatively and objectively. SWE has been used to evaluate the stiffness of liver and thyroid tissues and is a well-established technique for measuring liver elasticity.¹¹⁻¹⁷

Several studies have confirmed that the SWV reflects the thyroid tissue stiffness, and that the SWE is

This is an open access article under the terms of the Creative Commons Attribution-NonCommercial-NoDerivs License, which permits use and distribution in any medium, provided the original work is properly cited, the use is non-commercial and no modifications or adaptations are made.

From the Department of Otolaryngology, Head and Neck Surgery (T.F., E.M., R.D., S.K., N.M., K.F., H.T.), Tottori University Faculty of Medicine, Yonago, Japan

Editor's Note: This Manuscript was accepted for publication 2 April 2018.

This manuscript was presented on the podium at the 3rd World Congress of Thyroid Cancer at Westin Boston Waterfront, Boston, Massachusetts, July 27-30, 2017.

#Send correspondence to Takahiro Fukuhara, MD, PhD, 36-1 Nishicho, Yonago, Tottori, 683-8504, Japan. Email: tfukuhara3387@med.tottori-u.ac.jp

DOI: 10.1002/liv.2.165

useful for differentiating malignant from benign thyroid nodules.^{13–16} However, the correlation between strain imaging (ARFI imaging and strain elastography [SE]) and SWE remains unclear.

In this study, we measured the diagnostic accuracy of ARFI imaging for differentiating malignant thyroid nodules and established its usefulness by comparing ARFI imaging to conventional elastography. Furthermore, to verify the correlation between the ARFI imaging score proposed in this study and thyroid tissue stiffness, we assessed the stiffness of thyroid nodules with each score of ARFI imaging using SWV measurements.

PATIENTS AND METHODS

This study was approved by the ethics committee and institutional review board of Tottori University. Informed consent was obtained from patients and the study met the ethical guidelines of the Helsinki Declaration.

Patient Tissue Samples

Two hundred sixty-six thyroid nodules from 236 patients were examined by ultrasonography (US) between August 2014 and July 2016. Patients had undergone conventional SE, ARFI imaging, and SWE. Twenty-three nodules from 22 patients were excluded due to lack of disease pathology by fine needle aspiration biopsy (FNAB) or surgery. The remaining 243 thyroid nodules from 214 patients revealed disease cytology or pathology with fine needle aspiration biopsy/surgery and were subsequently examined in this study. The following circumstances excluded specific patient specimens from our analysis: ARFI imaging was not performed (one patient); pathological confirmation was not obtained in thyroid nodules (one patient had unsatisfactory tissue samples, and four patients presented with atypia of undetermined significance in their FNA results); a large nodule included surrounding tissue within the region of interest (ROI) (two patients); the nodule underwent percutaneous ethanol injection therapy (one patient); and one patient with lung cancer exhibited a metastatic nodule. Thus, 10 nodules from 10 patients were excluded. In total, 233 nodules from 204 patients were examined in this study (Fig. 1).

Ultrasound System

Each neck scan was performed with the Acuson S2000 ultrasound system (Siemens Medical Solutions, Mountain View, CA, USA) using a 14-MHz linear transducer for B-mode scan and flow imaging and 9L4 linear transducer for Elastography.

Ultrasonography Examination

All patient examinations were performed by two head and neck surgeons and one sonographer. One surgeon had over 10 years of experience performing thyroid US and over five years of experience performing thyroid elastography. The other surgeon had over five years of experience performing both thyroid US and elastography. One sonographer had over five years of experience performing both thyroid US and elastography. All patients were scanned in supine positions with their necks slightly extended. The thyroid nodules were evaluated by US in both transverse and longitudinal directions. For elastography, transverse scans were performed following the World

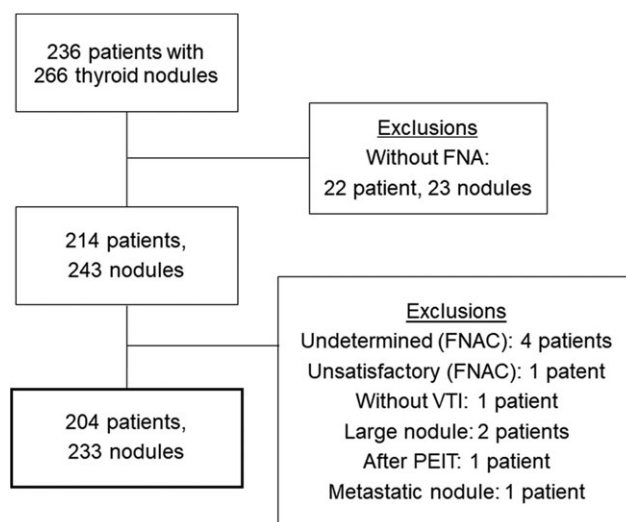


Fig. 1. Flowchart of patient selection during this study. FNA = fine needle aspiration; FNAC = fine needle aspiration cytology; PEIT = percutaneous ethanol injection therapy

Federation of Ultrasound in Medicine and Biology (WFUMB) recommendations.^{3,18,19}

Conventional SE

For conventional SE we used the eSie Touch system (Acuson S2000). This ultrasound application generates stress using carotid artery pulsation or physiological vibration of muscle and the default display depicts stiff tissue regions in blue color, soft tissue regions in red, and intermediate stiffness or strain regions in green. In our study, the transducer was held motionless, in light contact with the skin over the thyroid. The ROI was defined to include the nodule of interest and sufficient surrounding tissue: thyroid parenchyma and strap muscles. We adopted the WFUMB recommendations for indicating SE image quality, including the use of three images of SE with strain quality indicator >50 for each nodule.^{3,20,21} In order to score strain histograms, we adopted the four-point scoring system.^{22,23} The four-point system is as follows: score 1, the nodule is entirely green; score 2, the nodule is mostly green, with some blue areas; score 3, the nodule is mostly blue, with some green areas; score 4, the nodule is entirely blue.

In cases of discordance between the three images, the final decision was reached by consensus among the examiners.

ARFI imaging

The Virtual Touch Imaging (VTI) system (Acuson S2000) was used for strain elastography by means of ARFI imaging. The transducer was held motionless, in light contact with the skin over the thyroid in a transverse position. The ROI was defined to include the nodule and sufficient surrounding tissue: thyroid parenchyma and strap muscles. The ARFI imaging was performed three times at the same location and was assessed with a four-point classification system. The four-point system of VTI is as follows: score 1, the nodule is white or white honeycomb colored (lighter than surrounding tissue); score 2, the nodule is light gray (similar to a thyroid parenchyma); score 3, the nodule is dark gray (darker than surrounding tissue); score 4, the nodule is black (Fig. 2).

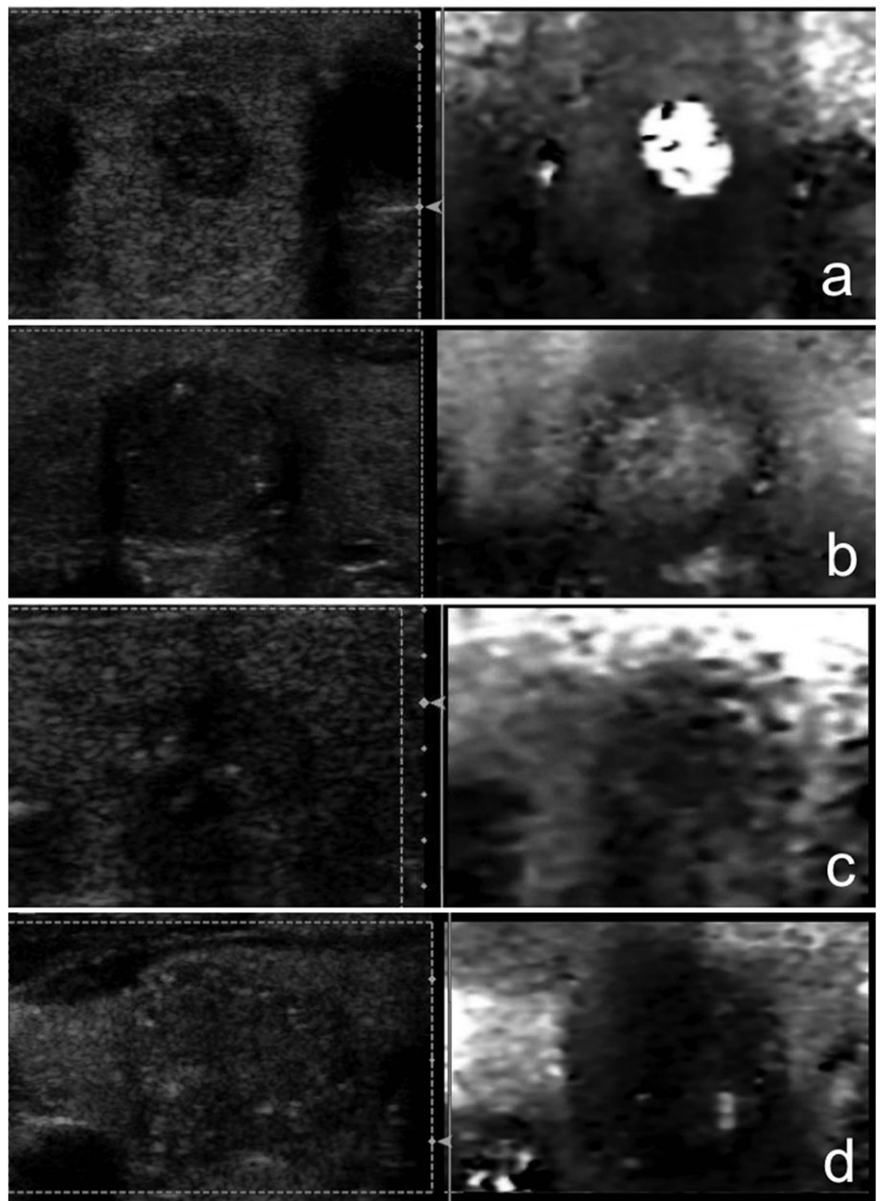


Fig. 2. Four-pattern scoring system of VTI (B-mode [left side] and ARFI imaging [right side] images)

a. Score 1: the nodule is white or white honeycomb (lighter than the surrounding tissue); b. Score 2: the nodule is light gray (similar in color to a thyroid parenchyma); c. Score 3: the nodule is dark gray (significantly darker than surrounding tissue); d. Score 4: the nodule is black.

Only the content of each nodule was measured and assessed by ARFI imaging, not the outer capsule. For example, a nodule whose content was measured and represented as light gray in color with a black capsule was assessed as VTI score 2 (light gray). If a nodule was represented with mostly black color and white dots, the color of this solid lesion was scored as VTI score 4 (black). In cases of discordance between the three images, the final decision was reached by consensus among the examiners.

Shear Wave Elastography

The Virtual Touch Quantification system (Acuson S2000) was used as SWE. The velocity of the shear wave generated by ARFI within a tissue reflects the stiffness within the tissue. Thus, SWE can be used to evaluate tissue stiffness, both quantitatively and objectively as used for the assessment of liver fibrosis.^{11,12} In this study, we assessed thyroid nodule stiffness using SWE.

The 5 mm × 5 mm ROI was completely circumscribed by the thyroid nodule. Five measurements were performed at the

same location and the average of these measurements was calculated for each nodule.²⁴ If the measurements were “x.xx” m/s, we were unable to accurately measure the lesions and therefore did not include these data for those nodules.

First, we compared the results between SE and ARFI imaging and assessed the SWV of thyroid nodules with each SE and ARFI imaging score (VTI score) in order to verify that the scores reflected the stiffness of the thyroid nodules.

Second, we compared the diagnostic accuracy among examiners to assess the inter-observer variation.

Third, we divided the subjects based on their diameters: (nodules ≥ 1.5 cm, nodules < 1.5cm and ≥ 1.0 cm, and nodules < 1.0 cm) and compared the diagnostic accuracy among the three groups.

Statistical Analysis

Statistical analysis was performed using SPSS software, version 22 (IBM Corporation, NY, USA). The diameters of the

TABLE I.
Basic Characteristics of Patients and Nodules

	Benign	Malignant	P values	
Patients (n = 204)				
Age (mean ± SD)	62.0 ± 15.3	59.4 ± 15.1		
Sex (Male/Female)	34 / 125	12 / 33		
Nodules (n = 233)				
Pathological type	Nodular hyperplasia	158	Papillary carcinoma	42
	Follicular adenoma	46	Follicular carcinoma	3
			Medullary carcinoma	1
			Anaplastic carcinoma	4
Longest diameter (mm)	24.0 ± 18.7	19.3 ± 13.7	.009**	
Transverse diameter (mm)	19.8 ± 11.4	16.2 ± 11.4	.005**	

nodules were compared using the Mann–Whitney U test. The sensitivity, specificity, positive predict value (PPV), negative predict value (NPV), and diagnostic accuracy of conventional SE and ARFI imaging for malignant nodules were calculated with the chi-square test. The SWV outcomes of VTI and SE scores were compared with the Kruskal–Wallis test and subjected to post-hoc comparison.

RESULTS

The basic characteristics of the patients and thyroid nodules are indicated in Table I. Of the 233 thyroid nodules examined, 183 were benign and 50 were malignant. The malignant nodules included 42 papillary carcinomas, three follicular carcinomas, four anaplastic carcinomas, and one medullary carcinoma. The longest and transverse diameters of benign nodules were significantly larger than those of malignant nodules.

Conventional SE

Nine nodules were examined without the assessment by conventional SE. Upon using conventional SE, the SE scores of benign nodules were as follows: 67 nodules of score 1, 49 nodules of score 2, 47 nodules of score

3, and 12 nodules of score 4 (Table II). The SE scores of malignant nodules were as follows: 8 nodules of score 1, 10 nodules of score 2, 19 nodules of score 3, and 12 nodules of score 4 (Table II). SE scores of 3 and 4 were highly predictive of malignancy ($P < .001$). When the nodules with SE score ≥ 3 were determined as malignant as previously reported,^{22,23} the sensitivity, specificity, PPV, NPV, and diagnostic accuracy were determined to be, respectively, 63.2%, 66.3%, 34.4%, 86.6%, and 65.6% (Table III).

ARFI Imaging

When ARFI imaging was employed, the VTI scores of benign nodules were as follows: 41 nodules of score 1, 117 nodules of score 2, 22 nodules of score 3, and 3 nodules of score 4 (Table II). The VTI scores of malignant nodules were as follows: 2 nodules of score 1, 8 nodules of score 2, 16 nodules of score 3, and 24 nodules of score 4 (Table II). Of 183 benign nodules, 158 (86.3%) were classified into either VTI score 1 or 2; 40 of 50 (80.0%) malignant nodules were classified into either VTI score 3 or 4. This demonstrated that VTI scores of 3 and 4 were highly predictive of malignancy ($P < .001$) with a sensitivity of 80.0%, specificity of 86.3%, PPV of 61.5%, NPV of 94.0%, and diagnostic accuracy of 85.0% (Table III).

Overall, the diagnostic accuracy of ARFI imaging for malignant thyroid nodules was better than that of conventional SE.

TABLE II.
Numbers of the Nodules with each SE and VTI Score.

	SE score				Total
	Score 1	Score 2	Score 3	Score 4	
Benign	67	49	47	12	175
Malignant	8	10	19	12	49
	VTI score				Total
	Score 1	Score 2	Score 3	Score 4	
Benign	41	117	22	3	183
Malignant	2	8	16	24	50

VTI = Virtual Touch Imaging; SE = strain elastography.

TABLE III.
Comparison of the Abilities of Conventional SE and ARFI Imaging to Differentiate Malignant Thyroid Nodules

	Sensitivity	Specificity	PPV	NPV	Accuracy
Conventional SE	63.2%	66.3%	34.4%	86.6%	65.6%
ARFI imaging	80.0%	86.3%	61.5%	94.0%	85.0%

ARFI = Acoustic Radiation Force Impulse; NPV = negative predict value; PPV = specificity, positive predict value; SE = strain elastography.

TABLE IV.
VTI Score of Each Malignant Pathology.

	VTI score				Total
	Score 1	Score 2	Score 3	Score 4	
Papillary Ca	2	5	14	21	42
Follicular Ca	0	3	0	0	3
Medullary Ca	0	0	1	0	1
Anaplastic Ca	0	0	1	3	4
Total	2	8	16	24	50

VTI = Virtual Touch Imaging; Ca = carcinoma.

ARFI Imaging of Malignant Pathologies

After examining 10 malignant nodules of VTI scores of 1 or 2, three follicular carcinomas and seven papillary carcinomas were identified (Table IV). In the seven papillary carcinomas with VTI scores of 1 or 2, two were classified as follicular variant, one presented with a cystic lesion, and one with macrocalcification.

SWE

The median values of the SWVs for the nodules in each SE score were as follows: 1.75 m/s in score 1, 1.89 m/s in score 2, 1.82 m/s in score 3, and 2 m/s in score 4. There was no significant difference among SWVs for each SE score (Fig. 3A).

The median values of the SWVs for the nodules in each VTI score were as follows: 1.57 m/s in score 1, 1.73 m/s in score 2, 1.88 m/s in score 3, and 2.09 m/s in score 4. The SWVs in scores 3 and 4 were significantly higher than those in scores 1 and 2 (Fig. 3B).

The VTI score appeared to reflect the stiffness of the target nodules significantly more than the SE scores.

Inter-observer variation

One hundred twenty-six out of 233 nodules were examined by the senior surgeon, 17 by the junior

TABLE V.
The Sensitivities, the Specificities, PPVs, NPVs, and Diagnostic Accuracies of Each Group Based on Nodule Size

	< 1 cm (38 nodules)	< 1.5 cm and ≥ 1.0 cm (45 nodules)	≥ 1.5 cm (150 nodules)
The sensitivity	87.5%	90%	70.8%
The specificity	81.8%	80%	88.9%
PPV	77.8%	56.3%	54.8%
NPV	90%	96.6%	94.1%
Diagnostic accuracy	84.2%	82.2%	86%

NPV = negative predict value; PPV = specificity, positive predict value.

surgeon, and 90 by the sonographer. For malignant nodules, diagnostic accuracies were 84.1% for the senior surgeon, 94.1% for the junior surgeon, and 84.4% for the sonographer.

Diagnostic accuracy depends on the nodule size

The subjects were divided into groups based on nodule size: ≥ 1.5 cm, 150 nodules, (126 benign, 24 malignant); < 1.5 cm and ≥ 1.0 cm, 45 nodules (35 benign and 10 malignant); and < 1 cm, 38 nodules (22 benign and 16 malignant). The sensitivities, the specificities, PPVs, NPVs, and diagnostic accuracies of each group were shown in Table V.

DISCUSSION

In this study, the diagnostic accuracy of ARFI imaging was demonstrated as superior to conventional SE. We believe that conventional SE is unable to detect small differences in tissue stiffness because the transducer used in conventional SE generates a large amount of stress throughout the tissue. By contrast, ARFI imaging may be able to detect subtle differences in tissue stiffness because the focused acoustic push pulse stress locally targets tissues and micro-displacement of tissue can be detected with the detect pulse.

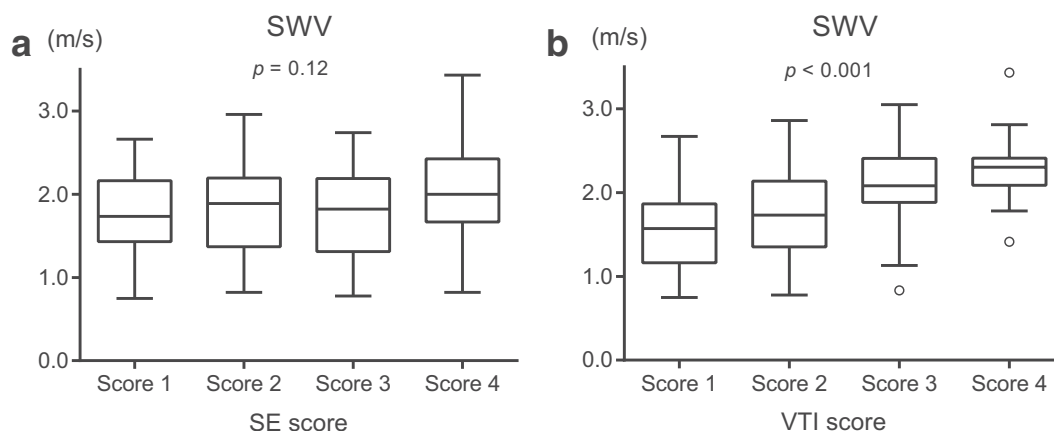


Fig. 3. A. Shear wave velocities (SWVs) of each SE score. There were no significant differences among the four scores ($P = .12$). Kruskal-Wallis Test.

B. SWVs of each VTI score. There were significant differences among the four scores ($P < .001$). Kruskal-Wallis Test.

Conventional SE uses operator-dependent manual compression and the strain change depends on the pressing force or speed.³ It is difficult to eliminate user subjectivity during the examination, because the examiner is responsible for selecting the appropriate color map images, introducing a significant source of potential user error depending on variable manual compression during the procedure. In addition, there are documented difficulties with reproducibility.^{2,3,20,24} As a result, conventional SE has a wide range of sensitivities (65–100%) and specificities (6–100%).^{4–9}

In contrast to conventional SE, new elastography methods using ARFI evaluate the fine displacement of tissue generated by an acoustic push pulse. ARFI imaging does not require manually moving a transducer; the transducer is instead held in place in light contact with the skin. The examiners only produce one image per measurement; thus, they will obtain the same image regardless of their experience with this technique. Therefore, ARFI imaging appears to be capable of assessing the local elastic characteristics of target tissues in an objective manner. In fact, in this study, diagnostic accuracy did not differ among examiners. This result demonstrates that the results of examination by ARFI imaging are not operator-dependent.

The five- and four-pattern scoring systems were reported as conventional SE scoring systems. In 2006, the Tsukuba five-pattern visual scoring system was reported for thyroid nodules.²⁵ In Rago et al., the authors rearranged the scoring system into a four-pattern scoring system. This system is easy to use and has been adopted for use worldwide.^{22,23}

In this study, the sensitivity (63.2%) and specificity (66.3%) of SE were lower than those of previous meta-analyses using the four-point scoring system whose sensitivity and specificity were 79–86% and 66.7–82%.^{26–28} One reason for this disparity may be that we selected the SE images based on a strain quality indicator of >50 rather than the image color because we wanted to eliminate user subjectivity in this study. All images that contained artifacts were eliminated from our analyses.

Unfortunately, there are few studies that use ARFI imaging for the thyroid. Thus, there is no fixed scoring system. Zhang et al. reported a six-pattern scoring system that is cited in a previous report, but is limited in that it was developed by a single study group.²⁹ This six-pattern scoring system is difficult to use for classification, as it relies on determining the ratio of light to dark gray, which can be challenging to distinguish using a grayscale image.²⁹ ARFI imaging measures the displacement of the tissue generated by push pulse and represents the extent of displacement with a grayscale, which can pose a problem because the surrounding thyroid parenchyma is also represented in grayscale colors. In addition, classification using six grades (dark portion, then 0–20%, 20–40%, 40–60%, 60–80%, 80–99%, and 100% light portion) was difficult.

Because of these complications, we adapted a four-point scoring system for ARFI imaging purposes. The four-point scoring system evaluates each nodule in comparison with surrounding thyroid parenchyma and is

easy to recognize. Zhang et al. reported a four-point scoring system for VTI classification of liver tissue,^{30–32} which is similar to our scoring system.

In this study, we identified 10 malignant nodules with VTI scores of 1 or 2. The pathologies of three nodules indicated follicular carcinomas and three indicated papillary carcinoma follicular variants. They were follicular structures without fibrosis. We believe that one malignant nodule was actually a macro-calcification and another a large cyst, and were classified into scores 1 and 2 because of these artifacts.

SWE has been well regarded for its ability to assess liver fibrosis.^{11,12} SWE has also been used to assess fibrotic stiffness in the thyroid region.^{14–16} The SWVs of nodules classified as VTI scores 3 and 4 were significantly higher than those of VTI scores 1 and 2. Regarding conventional SE, there is only a significant difference between SE score 4 nodules and the other nodules (SE scores 1–3). This suggests that ARFI imaging is more sensitive than conventional SE.

The diagnostic accuracies of ARFI imaging for the three size groups of thyroid nodules were broadly similar. In the American Thyroid Association Management Guideline or thyroid imaging reporting and data system (TIRADS), the decision about whether to perform fine needle aspiration (FNA) on thyroid nodules <1.5 cm and ≥1.0 cm depends on their B-mode features. ARFI imaging can supplement decision-making about whether to perform FNA for nodules <1.5 cm and ≥1.0 cm. Furthermore, ARFI imaging can reveal nodules <1.0 cm, which should be observed carefully. Additionally, ARFI imaging may be useful for choosing a nodule that has a risk of malignancy from among many adenomatous nodules.

Limitations

We realize that this study had limitations. First, the majority of malignant nodules were papillary carcinomas. However, papillary carcinomas are the majority of thyroid nodules in patient populations. Second, there is a possibility that the follicular adenomas in this study included follicular carcinoma. However, even if follicular carcinomas were included, there were very few of them. Third, there were a few nodules for which the SWV could not be measured. Fourth, we did not perform a comprehensive review of the pathology for each nodule. Fifth, since ARFI imaging is a novel technique, we may not have performed optimal operation of this technique. Sixth, we were unable to fully eliminate user subjectivity, as VTI scores were chosen by reviewers.

CONFLICT OF INTEREST

The authors have no conflict of interest to declare.

Acknowledgments

This work was supported by JSPS KAKENHI Grant Number 16K20246.

BIBLIOGRAPHY

1. Lyshchik A, Higashi T, Asato R, et al. Thyroid gland tumor diagnosis at US elastography. *Radiology* 2005;237(1):202–211.
2. Park SH, Kim SJ, Kim EK, Kim MJ, Son EJ, Kwak JY. Interobserver agreement in assessing the sonographic and elastographic features of malignant thyroid nodules. *AJR Am J Roentgenol* 2009;193(5):W416–23.
3. Cosgrove D, Barr R, Bojunga J, et al. WFUMB guidelines and recommendations on the clinical use of ultrasound elastography: PART 4. Thyroid. *Ultrasound Med Biol* 2017;43(1):4–26.
4. Rago T, Santini F, Scutari M, Pinchera A, Vitti P. Elastography: new developments in ultrasound for predicting malignancy in thyroid nodules. *J Clin Endo Metab* 2007;92(8):2917–2922.
5. Tranquart F, Bleuzen A, Pierre-Renault P, Chabrolle C, Sam Giau M, Lecomte P. Elastasonography of thyroid lesions. *J Radiol* 2008;89(1):35–39.
6. Lippolis PV, Tognini S, Materazzi G, et al. Is elastography actually useful in the presurgical selection of thyroid nodules with indeterminate cytology? *J Clin End Metab* 2011;96(11):1826–1830.
7. Moon HJ, Sung JM, Kim EK, Yoon JH, Youk JH, Kwak JY. Diagnostic performance of gray-scale US and elastography in solid thyroid nodules. *Radiology* 2012;262(3):1002–1013.
8. Azizi G, Keller J, Lewis M, Puett D, Rivenbark K, Malchoff C. Performance of elastography for the evaluation of thyroid nodules: a prospective study. *Thyroid* 2013;23(6):734–740.
9. Ko SY, Kim EK, Sung JM, Moon HJ, Kwak JY. Diagnostic performance of ultrasound and ultrasound elastography with respect to physician experience. *Ultrasound Med Biol* 2014;40(5):854–863.
10. Benson J, Fan L. Tissue strain analysis: a complete ultrasound solution for elastography. Medical Solutions—Siemens Healthcare Global. www.healthcare.siemens.com/. Accessed November 20, 2011.
11. Sporea I, Sirlir R, Popescu A, Danilă M. Acoustic radiation force impulse (ARFI)—a new modality for the evaluation of liver fibrosis. *Med Ultrason* 2010;12(1):26–31.
12. Friedrich-Rust M, Nierhoff J, Lupsor M, et al. Performance of acoustic radiation force impulse imaging for the staging of liver fibrosis: a pooled meta-analysis. *J Viral Hepat* 2012;19(2):212–219.
13. Fukuhara T, Matsuda E, Fujiwara K, et al. Phantom experiment and clinical utility of quantitative shear wave elastography for differentiating thyroid nodules. *Endocrine J* 2014;61(6):615–621.
14. Fukuhara T, Matsuda E, Endo Y, et al. Correlation between quantitative shear wave elastography and pathological structure of thyroid lesions. *Ultrasound Med Biol* 2015;41(9):2326–2332.
15. Fukuhara T, Matsuda E, Izawa S, Fujiwara K, Kitano H. Utility of shear wave elastography for diagnosing chronic autoimmune thyroiditis. *J Thyroid Res* 2015;2015:164548. doi: 10.1155/2015/164548.
16. Fukuhara T, Matsuda E, Endo Y, et al. Impact of fibrotic tissue on shear wave velocity in thyroid: An ex vivo study with fresh thyroid specimens. *Biomed Res Int* 2015;2015:569367. doi: 10.1155/2015/569367.
17. Grahzani H, Cantisani V, Lodise P, et al. Prospective evaluation of acoustic radiation force impulse technology in the differentiation of thyroid nodules: accuracy and interobserver variability assessment. *J Ultrasound* 2014;17(1):13–20.
18. Bhatia KS, Tong CS, Cho CC, Yuen EH, Lee YY, Ahuja AT. Shear wave elastography of thyroid nodules in routine clinical practice: preliminary observations and utility for detecting malignancy. *Eur Radiol* 2012;22(11):2397–2406.
19. Hou XJ, Sun AX, Zhou XL, et al. The application of Virtual Touch tissue quantification (VTQ) in diagnosis of thyroid lesions: A preliminary study. *Eur J Radiol* 2013;82(5):797–801.
20. Calvete AC, Rodriguez JM, de Dios Berná-Mestre J, Ríos A, Abellán-Rivero D, Reus M. Interobserver agreement for thyroid elastography: Value of the quality factors. *J Ultrasound Med* 2013;32(3):495–504.
21. Cappelli C, Pirola I, Gandossi E, et al. Real-time elastography: A useful tool for predicting malignancy in thyroid nodules with nondiagnostic cytologic findings. *J Ultrasound Med* 2012;31(11):1777–1782.
22. Rago T, Di Coscio G, Basolo F, et al. Combined clinical, thyroid ultrasound and cytological features help to predict thyroid malignancy in follicular and Hürthle cell thyroid lesions: Results from a series of 505 consecutive patients. *Clin Endocrinol (Oxf)* 2007;66(1):13–20.
23. Rago T, Vitti P. Role of thyroid ultrasound in the diagnostic evaluation of thyroid nodules. *Best Pract Res Clin Endocrinol Metab*. 2008;22(6):913–28.
24. Sporea I, Sirlir R, Bota S, Vlad M, Popescu A, Zosin I. ARFI elastography for the evaluation of diffuse thyroid gland pathology: Preliminary results. *World J Radiol* 2012;4(4):174–178.
25. Itoh A, Ueno E, Tohno E, et al. Breast disease: Clinical application of US elastography for diagnosis. *Radiology* 2006;239(2):341–350.
26. Ghajarzadeh M, Sodagari F, Shakiba M. Diagnostic accuracy of sonoelastography in detecting malignant thyroid nodules: A systematic review and meta-analysis. *AJR Am J Roentgenol* 2014;202(4):W379–W389.
27. Sun J, Cai J, Wang X. Real-time ultrasound elastography for differentiation of benign and malignant thyroid nodules: a meta-analysis. *J Ultrasound Med* 2014;33(3):495–502.
28. Razavi SA, Haddock TA, Sadigh G, Dwamena BA. Comparative effectiveness of elastographic and B-mode ultrasound criteria for diagnostic discrimination of thyroid nodules: a meta-analysis. *AJR Am J Roentgenol* 2013;200(6):1317–1326.
29. Zhang YF, He Y, Xu HX, et al. Virtual Touch tissue imaging of acoustic radiation force impulse: a new technique in the differential diagnosis between benign and malignant thyroid nodules. *J Ultrasound Med* 2014;33(4):585–595.
30. Zhang FJ, Han RL, Zhao XM. The value of virtual touch tissue image (VTI) and virtual touch tissue quantification (VTQ) in the differential diagnosis of thyroid nodules. *Eur J Radiol* 2014;83(11):2033–2040.
31. Zhang F, Zhao X, Han R, Du M, Li P, Ji X. Comparison of acoustic radiation force impulse imaging and strain elastography in differentiating malignant from benign thyroid nodules. *J Ultrasound Med* 2017;36(12):2533–2543.
32. Shuang-Ming T, Ping Z, Ying Q, Li-Rong C, Ping Z, Rui-Zhen L. Usefulness of acoustic radiation force impulse imaging in the differential diagnosis of benign and malignant liver lesion. *Acad Radiol* 2011;18(7):810–815.